

$\rho_c$ : コークスの嵩比重逆数  $m^3/kg$

ここでは  $O/C=2.5$  として  $W=600 kg/m^3$  について計算した。

計算結果と実験結果にはいくらか差があるが、サンプリングや分析など誤差が生じやすい点があり、傾向的に一致しているとみられる。

このような計算を高炉にあてはめるにはまだ幾多の問題が残っており、さらに複雑な計算を行なわねばならない。しかしこの程度の計算によつても、コークス比に最も大きな影響を与える間接還元の状態に関し、多くの示唆に富む結果を得ることができると考えられるので、今後種々の操業条件、原料条件について検討を加える予定である。

5. 結 言

高炉シャフト部の間接還元を知るためのアプローチとして小型シャフト炉における還元状態を計算によつて求め、実験と比較した結果、

1) 化学反応律速に基く次の還元反応速度式によつてシャフト炉内の還元を計算することができる。

$$D(1 - \sqrt[3]{1 - y}) = K(CO - CO_2Ce)T \cdot \exp(-\Delta H/RT) \cdot t$$

2) 界面における反応としては  $700^\circ C$  以上で  $FeO \rightarrow Fe$  を考えればよい。

3) 低温における  $Fe_2O_3 \rightarrow Fe_3O_4$  の反応は極めて早いことを認めた。

文 献

- 1) 児玉, 重見, 堀尾: 鉄と鋼, 49 (1963) 10, p. 1299
- 2) 小菅, 児玉, 堀尾, 稲垣: 鉄と鋼, 52 (1966) 3, p. 310
- 3) 児玉, 重見, 東: 鉄と鋼, 47 (1961) 3, p. 271
- 4) J. O. EDSTRÖM: J. Iron & Steel Inst. (U. K.), 175 (1953), p. 289
- 5) V. J. MORAN and A. E. JENKINS: J. Iron & Steel Inst. (U. K.), 199 (1961), p. 26
- 6) K. H. URLICH and K. BOHNENKAMP: Arch. Eisenhüttenw., 36 (1965), p. 611

(54) 酸化鉄還元過程の考察

(小型高炉による製鉄過程に関する基礎研究—II)

東京大学, 大学院

○フェリッポ・カルデロン

東京大学, 生産技術研究所 大 蔵 明 光

東京大学, 工学部 工博 松 下 幸 雄

Considerations of Iron Reduction Processes.

(Basic study on iron making by a miniature blast furnace—II)

Felipe P. CALDERON, Akimitsu OHKURA and Dr. Yukio MATSUSHITA.

1. Introduction

This paper is with reference to an earlier paper<sup>1)</sup>. The same furnace was used with some modifications made particularly in the smelting zone and in the

hearth region. The furnace condition with regards to blast volume and temperature, were very close to those of the earlier operations. In the present paper, additional data are provided on the partial reduction, change of  $Fe^{3+}$ ,  $Fe^{2+}$ , Fe content along the shaft, silicon and carbon content of the crude metal. The principal object of this paper is to investigate the gas distribution with change of ore/coke ratio.

2. Experimental Procedure

The method of operation<sup>1)</sup>, the volumetric chemical analysis, the x-ray and microscopic analysis of the solid samples were the same as those in the previous operations<sup>1)</sup>. In the present investigation, the ore/coke ratio was changed at certain period and gas samples were obtained at each interval and each change of ore/coke ratio. The gas samples were analyzed by use of a gas chromatograph of the kathometer type.

3. Results and Discussion

From the results of the volumetric chemical analysis, an equation was derived expressing the progress of reduction from the higher levels down to the smelting zone. From the same analysis, the  $Fe^{3+}$ ,  $Fe^{2+}$ , and Fe content along the shaft were obtained. Apparently, the degree of reduction is a function of various factors and conditions, although temperature could play a very important factor. As shown in Fig. 1, there is a marked difference between the degree of reduction of the two operations. The dependence of reduction with temperature is very ably demonstrated by A. Ohkura in his investigation<sup>2)</sup> on reductio) rate of iron ores in the fluidized bed reactor.

The x-ray and microscopic analysis gave similar results as to the progress of reductions along the shaft. Fig. 2 shows the progress of reduction indicated by

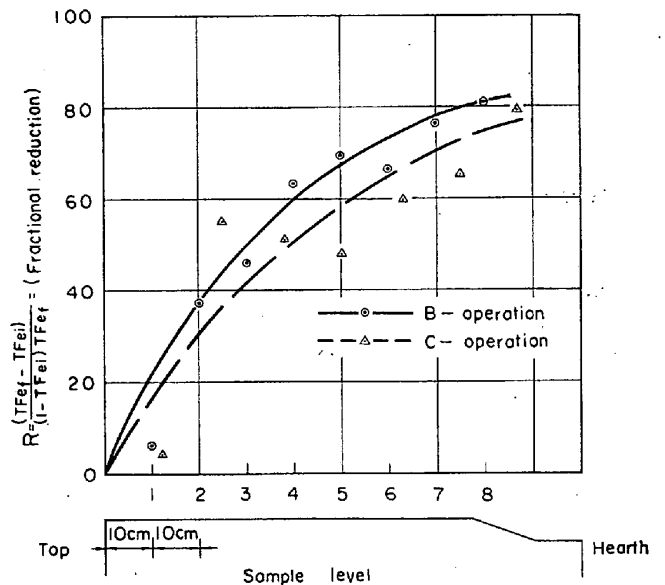


Fig. 1. The progress of fractional reduction down the furnace shaft.

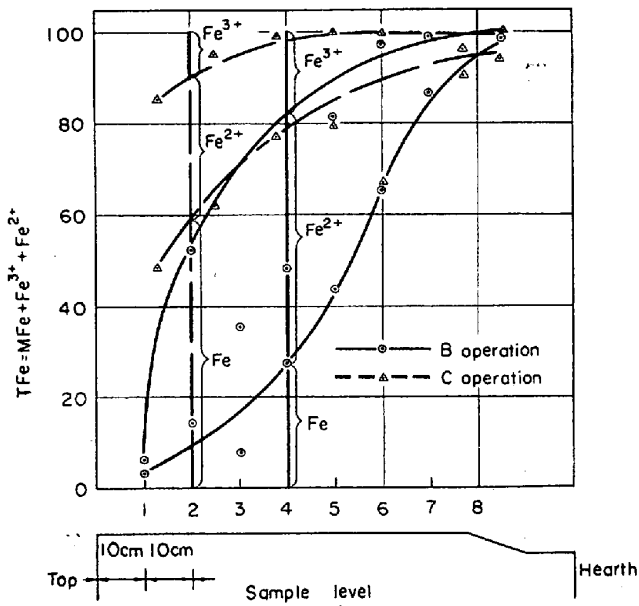


Fig. 2. The change of Fe<sup>3+</sup>, Fe<sup>2+</sup>, Fe down the furnace shaft.

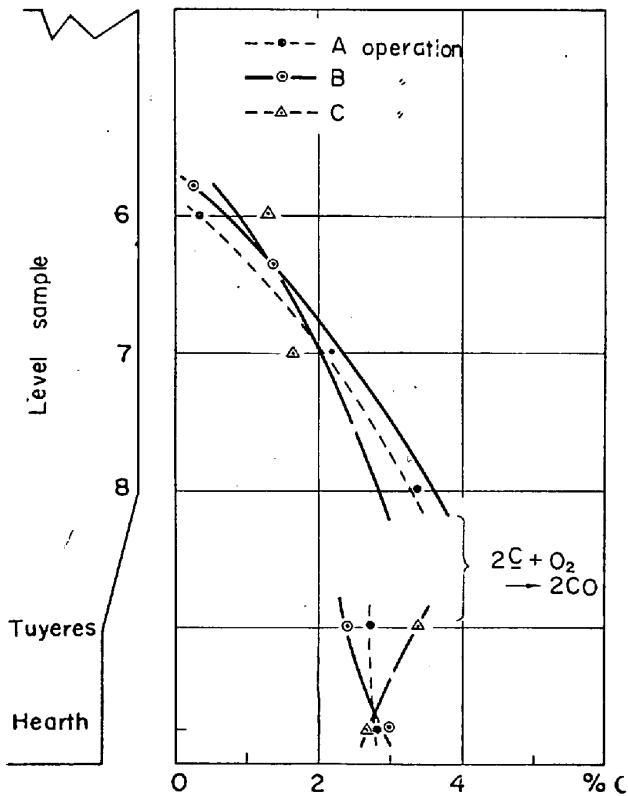
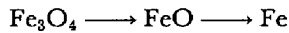


Fig. 3. Carbon content of samples at different level.

the change of Fe content as mentioned above. The reduction proceeds as follows:



The co-existence of Fe<sub>3</sub>O<sub>4</sub>, FeO and Fe observed under the microscope, notably those above the combustion zone, is a clear indication that iron oxide reduction is a reaction limited by CO/CO<sub>2</sub> ratio and temperature.

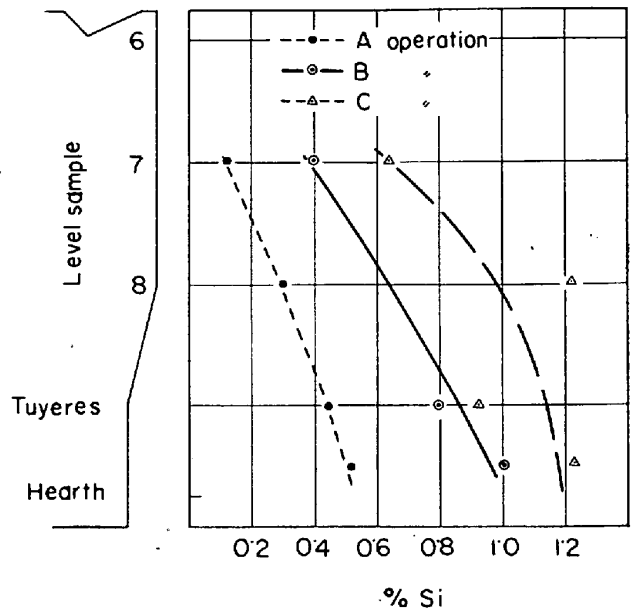


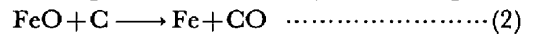
Fig. 4. Silicon content of samples at different level.

This is due to the difference of the oxygen potential of the oxides of iron at different temperature levels.

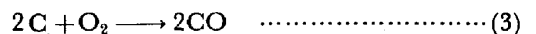
When the carbon monoxide gas gets in touch with the charge in the upper part of the furnace, it is cooled and forms carbon dioxide and free carbon.



This carbon in the form of fine powder and soot were found deposited on the furnace walls, some obviously penetrated into the porous ores, and at the higher temperature regions, reduced any remaining oxide.

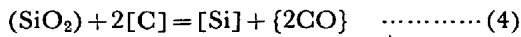


Solid samples obtained above the boshes were spongy mass of iron. This is because the remaining carbon was dissolved and consequently lowered the melting temperature. Coke extended down into the hearth. Intermingled metals and coke suggest that the molten metal ran through the coke making it saturated with carbon. It is to be expected therefore that carbon content increases down to the hearth. But due to the great velocity of the blast and the excess of oxygen used and the resulting turbulence in the boshes oxidation of dissolved carbon was enhanced.



The decrease of carbon content at the tuyere level is shown in Fig. 3.

It will be noted that the direct reduction of iron oxide is highly endothermic and is therefore favored by a high temperature. On the other hand, the reduction of the other metalloids such as silicon, manganese and phosphorous are even more endothermic. Silica is reduced to a certain extent in the smelting zone resulting in a proportion of silicon in iron. The reduction of silica can be illustrated according to the over all reaction:



$$K = \frac{[a_{\text{Si}}] \cdot P_{\text{CO}}^2}{[a_{\text{SiO}_2}] \cdot [a_{\text{C}}^2]} \quad \dots\dots\dots(5)$$

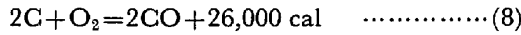
$$G = 161,500 - 87 \cdot 4T \quad \dots\dots\dots(6)$$

$$\log K = 19 \cdot 1 - \frac{35,300}{T} \quad \dots\dots\dots(7)$$

As would be expected from the temperature dependence of the equilibrium constant, the silicon content of the metal increases rapidly with increasing temperature. This is shown in Fig. 4.

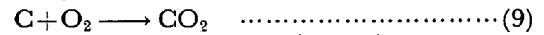
Fig. 5 gives a summary of the gas distribution along the shaft of the miniature furnace. Results are those obtained along the center line and those adjacent to the in-wall of the stack.

As soon as the air and coke meet, at the tuyeres combustion takes place.

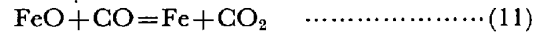
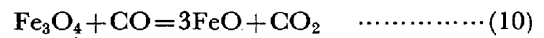


It is this CO that is responsible for the reduction of

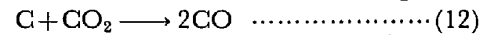
oxides in the upper part of the furnace. Theoretically from equation (8), it can be shown that the maximum amount of CO would be about 34.7% and little or no CO<sub>2</sub> is formed. In this investigation, it was found that about 5% CO<sub>2</sub> is present at the tuyere zone. This high content of CO<sub>2</sub> is due to the reaction of carbon and oxygen, the latter being used in excess and with a velocity higher than those of a commercial furnace.



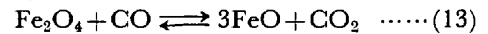
Generally, the tendency of the ascending furnace gas composition is an increase in CO content and decrease of CO<sub>2</sub> content. This is contrary to the fact that more CO<sub>2</sub> is formed as the ascending gas meets more and more oxide as illustrated in the following reactions:



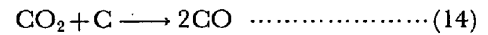
and in addition, the velocity of the reaction shown below is decreasing since this is an endothermic reaction and therefore a function of temperature.



It is highly probable that the phenomena encountered in this investigation is due to the following reasons:



Equation (13) is reversible and a function of temperature. The temperature of the gas samples were in the neighborhood of 1200~1500°C. The CO<sub>2</sub> formed as shown in equation (13) could have been directly reduced by carbon, the latter being used in excess, shown in equation (14)



Also, since the upward velocity of the stream of gases is comparatively rapid, any CO<sub>2</sub> formed but unreduced by carbon is quickly removed from the reacting phase thus reducing the concentration of CO<sub>2</sub> in the reacting zone.

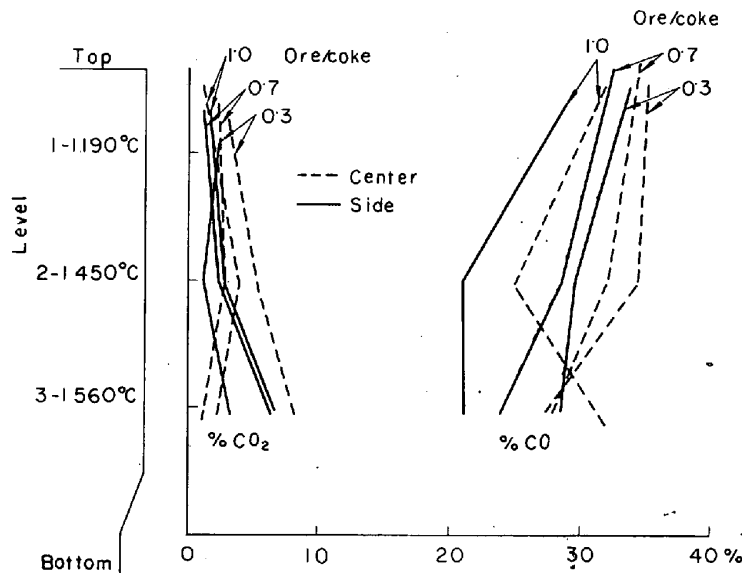


Fig. 5. Gas distribution with change of ore/coke ratio.

Table 1. Gas analysis.

Ore/Coke	Coke ratio	Sample	%CO		%CO <sub>2</sub>		CO/CO <sub>2</sub>		$\frac{P_{\text{CO}}}{P_{\text{CO}} + P_{\text{CO}_2}}$	
			Side	Center	Side	Center	Side	Center	Side	Center
0.3	5,880	1	33.60	35.40	2.37	3.65	14.20	9.70	0.9341	0.9065
		2	29.70	34.75	1.25	5.25	23.75	6.62	0.8866	0.9295
		3	28.55	27.10	3.10	7.82	9.20	3.46	0.9358	0.9536
0.7	2,520	1	18.40	33.80	1.90	2.50	9.68	13.52	0.9596	0.8687
		2	28.45	32.20	2.32	2.60	12.27	12.39	0.9247	0.9252
		3	23.10	28.35	6.35	1.20	3.64	23.60	0.8851	0.8609
1.0	1,760	1	28.35	31.30	1.94	1.52	14.60	20.60	0.9020	0.7760
		2	21.20	25.20	2.75	4.07	7.71	6.19	0.7860	0.9593
		3	21.35	31.90	6.50	2.69	4.39	11.86	0.7666	0.9222
1.0	1,760	Tuyere	7.85		5.22		1.5		0.6039	

The slight increase of  $\text{CO}_2$  with the increase of ore/coke ratio is to be expected as the system becomes more oxidizing atmosphere. It is very interesting to note that the gas composition in this investigation under the prevailing temperature are in the neighborhood of those found in the commercial blast furnace.

In a commercial furnace, reduction often proceed before a red heat zone is reached. Calculation of the oxygen potential of the gases from the results of gas analysis suggests that reduction occurred in the boundary of liquid oxide and delta iron. This finding is in agreement with the physical appearance of the samples obtained when the furnace was opened.

#### 4. Summary and Conclusion

$\text{Fe}_3\text{O}_4$ ,  $\text{FeO}$ , and  $\text{Fe}$  were found to be in wide range in the stack. Formation of vesicular thin shells of metal of varying sizes occurred in the melting zone. These thin shells enclosed tiny spherical mass of solid metal. Blast velocity and amount of oxygen affected the carbon content in the liquid iron at the combustion zone. Silicon, at low concentration is not re-oxidized, due to the close affinity of iron and silicon.

Theoretical calculation of material balance, heat balance, and amount of blast are indispensable guide for a smooth operation. When the blast volume was changed and ore the charge ratio varied, it considerably affected the stability of tapping time and fluidity of slag and amount of metal tapped.

The reducing power in a blast furnace is expressed by the  $\text{CO}/\text{CO}_2$  ratio and temperature. It appears here that the coke consumption and gas velocity seem to be the important controlling factors. The  $\text{CO}/\text{CO}_2$  ratio is very high, largely due to the high heat loss, but on the other hand, the amount of coke and velocity of the upstream of gases affected the amount of  $\text{CO}$  and  $\text{CO}_2$  at the reaction zone.

#### References

- 1) Akimitsu OHKURA, Felipe P. CALDERON, and Yukio MATSUSHITA: Tetsu to Hagane, 51 (1965) 10, p. 1769
- 2) Akimitsu OHKURA and Yukio MATSUSHITA: Tetsu to Hagane, 50 (1964) 2, p. 159

## (55) 高温熱風炉の昇温および操業経過について

三栄鉄工

安武正幸・園川峯喜・佐藤勝美  
森田治男・○笹川 浩

On the Heating-up and Operation of High Temperature Hot Stove.

Masayuki YASUTAKE, Mineki SONOKAWA,  
Katsumi SATO, Haruo MORITA  
and Hiroshi SASAGAWA.

### 1. 緒 言

三栄鉄工(株)第6次高炉改修工事にあつて、高炉送風温度  $1200^\circ\text{C}$  以上を目標としたため、既設の熱風炉2基のほかに、高温熱風炉(カウパー式)2基を増設した。同炉はドーム部および、チェッカー上部に珪石煉瓦を採用したので、乾燥昇温には慎重な熱風乾燥を行なつた。火入後送風温度は予熱熱風炉使用により、燃焼用空気を予熱し、またレキュペレーターにより、燃焼用Bガスを予熱することにより漸次上昇し、4月18日より  $1200^\circ\text{C}$  で操業を行なつている。その概要を2.以下に述べる。

### 2. 乾燥および昇温

#### 2.1 熱膨張

珪石煉瓦の高温における熱間性状は、他の耐火煉瓦に比較して、非常に安定しているが、低温時には  $\text{SiO}_2$  の結晶転移により、Fig. 1 に示すような容積膨張が起る。

#### 2.2 昇 温

高温熱風炉乾燥昇温にあつては、珪石煉瓦の加熱時における容積膨張を考慮して、既設旧熱風炉2基(伝熱面積  $3,500 \text{ m}^2/1$  基)を使用して重油燃焼によりチェッカーを加熱し、S 40年10月30日より27日間熱風乾燥を行なつた。

昇温速度は下記の通りである。

$100\sim 300^\circ\text{C}$ , —  $10\sim 20^\circ\text{C}/\text{day}$

$300\sim 900^\circ\text{C}$ , —  $40\sim 70^\circ\text{C}/\text{day}$

昇温経過を Fig. 2 に示す。

### 3. 操 業 実 績

11月25日火入後順調な操業を続けている。送風温度も

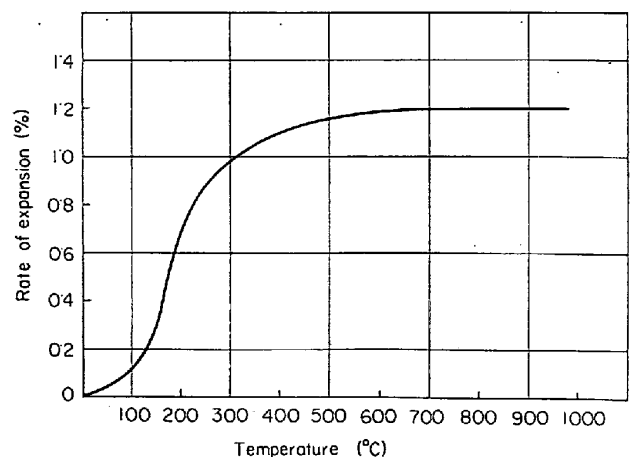


Fig. 1. Thermal expansion of silica brick.